



# Calendar- and Weather-Sensitive Short-Term Forecasting of Urban Bus Ridership: Evidence from the Transjakarta Bus Rapid Transit System



Hanifah Khairunnisa<sup>\*</sup>, Fellita Odelia Wibowo<sup>1</sup>, Gumgum Darmawan<sup>1</sup>

Department of Statistics, Universitas Padjadjaran, 45363 Sumedang, Indonesia

<sup>\*</sup> Correspondence: Hanifah Khairunnisa (hanifah22003@mail.unpad.ac.id)

**Received:** 12-18-2025

**Revised:** 02-19-2026

**Accepted:** 03-01-2026

**Citation:** H. Khairunnisa, F. O. Wibowo, and G. Darmawan, "Calendar- and weather-sensitive short-term forecasting of urban bus ridership: Evidence from the Transjakarta bus rapid transit system," *Mechatron. Intell Transp. Syst.*, vol. 5, no. 1, pp. 31–44, 2026. <https://doi.org/10.56578/mits050103>.



© 2026 by the author(s). Licensee Acadlore Publishing Services Limited, Hong Kong. This article can be downloaded for free, and reused and quoted with a citation of the original published version, under the CC BY 4.0 license.

**Abstract:** Urban public transport systems are required to respond to pronounced temporal variations in passenger demand driven by calendar effects, weather conditions, and evolving mobility patterns. Reliable short-term demand forecasts have therefore become an important role in supporting operational planning and service management in large-scale systems. This study examines the daily ridership dynamics of the Transjakarta bus rapid transit system and evaluates the forecasting performance of three modeling approaches: seasonal autoregressive integrated moving average with exogenous variables (SARIMAX), multilayer perceptron (MLP), and a dynamic moving-window model. The analysis is based on 851 daily observations from January 1, 2023 to April 30, 2025, with rainfall, working days, and national holidays included as exogenous variables. Each model is estimated using a training dataset and evaluated on a hold-out test set over a 30-day forecasting horizon. Forecast accuracy is assessed using the mean absolute percentage error (MAPE). The results indicate that the MLP model achieves the highest forecasting accuracy, with a MAPE of 8.547%, while SARIMAX and the dynamic model yield higher error levels of 33.345% and 37.754%, respectively. The findings suggest that non-linear modeling approaches are better suited to capturing the complex and irregular demand patterns observed in daily urban bus ridership data. The study provides empirical evidence that can support short-term planning and demand-aware operational decision-making in urban public transportation systems.

**Keywords:** Urban bus ridership; Short-term demand forecasting; Intelligent transportation systems; Seasonal autoregressive integrated moving average with exogenous variables; Multilayer perceptron

## 1 Introduction

Transportation systems in rapidly growing metropolitan areas face increasing pressure due to the imbalance between vehicle growth and the expansion of road infrastructure, leading to persistent congestion and reduced system efficiency [1]. Such conditions negatively affect travel time reliability and urban productivity [2], highlighting the need for efficient and sustainable public transport services. In Jakarta, the development of an integrated public transport network, including Mass Rapid Transit (MRT), Light Rail Transit (LRT), Commuter Line (KRL), and bus-based systems, reflects an ongoing policy effort to encourage modal shift from private vehicles to mass transit [3, 4]. Within this network, Transjakarta plays a central role as the primary bus rapid transit system, experiencing substantial growth in ridership from approximately 191 million passengers in 2022 to 371 million in 2024, alongside continuous route expansion into the surrounding Jabodetabek area [5–7].

Temporal variations in passenger demand represent a critical operational challenge for large-scale transit systems. For example, official statistics indicate that ridership declined in February 2025 due to a reduced number of working days, illustrating the influence of calendar effects on mobility patterns [8]. Such fluctuations are not necessarily associated with long-term changes in user preferences, but rather reflect short-term variations driven by working schedules, holidays, and external conditions. Reliable short-term demand forecasts are therefore essential for supporting service planning, fleet allocation, and timetable adjustments in urban public transportation systems.

Passenger demand dynamics are shaped by multiple external factors, including weather conditions, working days, and national holidays, which introduce irregular and non-linear variations into daily ridership patterns. Traditional univariate time series models, which rely solely on historical demand data, are often unable to capture the influence

of these exogenous factors, leading to limited forecasting accuracy under changing conditions [9, 10]. This motivates the use of multivariate and adaptive modeling approaches that explicitly incorporate external information into the forecasting process.

Seasonal autoregressive integrated moving average with exogenous variables (SARIMAX) models provide a statistical framework for representing seasonal structures while accounting for the influence of observable external variables such as rainfall and calendar effects [11]. However, the relationship between passenger demand and its influencing factors is often non-linear, which limits the explanatory and predictive capacity of linear models alone. Neural network-based approaches, such as the multilayer perceptron (MLP), are therefore applied to learn complex non-linear relationships from data and to improve short-term forecasting performance [12]. In addition, dynamic modeling approaches that update predictions using recent observations are useful for capturing short-term structural changes and evolving demand patterns in operational settings [13].

Previous work on Transjakarta ridership forecasting has largely relied on relatively simple techniques. For instance, Ikasari et al. [14] employed single exponential smoothing (SES) to forecast passenger volume on a specific corridor and reported a mean absolute percentage error (MAPE) of approximately 21%. While informative, such approaches do not incorporate exogenous variables or non-linear dynamics and are therefore limited in their ability to represent the full complexity of daily ridership fluctuations.

Against this background, the present study evaluates the performance of SARIMAX, MLP, and a dynamic moving-window model for short-term forecasting of daily Transjakarta ridership using calendar and weather-related exogenous variables. By comparing linear, non-linear, and adaptive approaches within a unified empirical framework, the analysis aims to provide evidence on the suitability of different modeling strategies for supporting demand-aware operational decision-making in urban public transportation and intelligent transportation systems.

## 2 Methodology

### 2.1 Data and Research Variables

The analysis is based on secondary data obtained from the Satu Data Jakarta portal, which serves as the official repository of transportation statistics for the city. The dataset titled “Number of Public Transport Passengers Served per Day” contains 851 daily observations covering the period from January 1, 2023, to April 30, 2025, providing a consistent daily time series for ridership analysis [15].

In addition to passenger volume, several exogenous variables are included to represent external conditions affecting daily travel behavior. These variables consist of daily rainfall (in millimeters) obtained from the Open-Meteo platform, a weekday indicator distinguishing working days from weekends, and a binary indicator for national holidays [16]. The weekday variable is coded as 1 for working days and 0 for weekends, while the holiday variable is coded as 1 for national holidays and 0 otherwise [17–19]. These variables reflect calendar and weather-related factors that are known to influence short-term public transport demand.

Prior to model estimation, the dataset was examined for completeness and internal consistency. No missing values were detected over the observation period, and therefore no imputation procedures were required. Given the uniform daily frequency of the data, no temporal aggregation or resampling was applied. Standard preprocessing steps, including variable alignment and formatting, were conducted to ensure compatibility with the forecasting models. Summary statistics of the variables are reported in Table 1.

**Table 1.** Daily data on the number of transjakarta passengers and related exogenous variables

Date	Number of Transjakarta Passengers	Rainfall (mm)	Weekday	National Holiday
01-01-2023	291030	21.8	0	1
02-01-2023	666777	11.8	1	0
03-01-2023	702891	14	1	0
04-01-2023	770560	7.2	1	0
05-01-2023	752938	0.8	1	0
26-04-2025	908279	7.3	0	0
27-04-2025	814411	3.2	0	0
28-04-2025	1272755	2.5	1	0
29-04-2025	1223516	1.5	1	0
30-04-2025	1163918	3.2	1	0

## 2.2 Data Characteristics

### 2.2.1 Data stationarity

To formally assess whether a time series exhibits long memory, one commonly used approach is the Geweke-Porter-Hudak (GPH) test. This test applies log-periodogram regression by regressing the logarithm of the periodogram spectrum on low frequencies in the Fourier domain. Mathematically, the parameter  $d$  is estimated through Eq. (1) [20].

$$\hat{d} = \frac{\sum_{j=1}^m (x_j - \bar{x})(y_j - \bar{y})}{\sum_{j=1}^m (x_j - \bar{x})^2} \quad (1)$$

With the following notation:

$$y_j = \ln I(\gamma_j), x_j = -\ln \left( 2 \sin \left( \frac{\gamma_j}{2} \right) \right)^2 \quad (2)$$

The hypotheses tested in the GPH test are:

$H_0 : \hat{d} = 0$  (no long memory/short memory detected)

$H_1 : \hat{d} \neq 0$  (long memory detected)

The interpretation of the value of  $d$  describes the memory characteristics of a time series. If  $d = 0$ , autocorrelation declines rapidly, indicating that the influence of past observations is limited to the short term. A value of  $0 < d < 0.5$  indicates stationary long memory, with autocorrelation that decreases slowly but remains stable. Meanwhile,  $d \geq 0.5$  indicates non-stationary long memory.

### 2.2.2 Seasonal pattern identification

Seasonal pattern detection in the data is performed using spectral regression, which represents the time series as a combination of sine and cosine functions at Fourier frequencies. This approach is used to identify hidden periodicities that cannot be directly observed in the time domain. The mathematical model is expressed in Eq. (3) [21, 22].

$$Z_t = \sum_{k=0}^{\lfloor n/2 \rfloor} (a_k \cos \omega_k t + b_k \sin \omega_k t) + e_t \quad (3)$$

After the Fourier parameters ( $a_k$  dan  $b_k$ ) are estimated, a hypothesis test is conducted to determine the presence of seasonal patterns, with the hypotheses and test statistics described accordingly.

$H_0 : a_k = \beta_k = 0$  (the data are not influenced by seasonal factors)

$H_1 : a_k \neq 0$  atau  $\beta_k \neq 0$  (the data are influenced by seasonal factors)

The F-test statistic is presented in Eq. (4).

$$F = \frac{(n-3)(a_k^2 + b_k^2)}{2 \sum_{j=1; j \neq k}^{\lfloor n/2 \rfloor} a_j^2 + b_j^2} \sim F(2, n-3) \quad (4)$$

Next, the dominant seasonal period is identified using the T-statistic, which compares the maximum ordinate of the periodogram to the total frequency energy, and is expressed mathematically in Eq. (5).

$$T = \frac{I^{(I)}(\omega_{(I)})}{\sum_{k=1}^{n/2} I(\omega_k)} \quad (5)$$

Frequencies with  $T_{\text{stat}}$  values exceeding the critical threshold  $g$  are interpreted as significant seasonal periods in the data.

The spectral method employed is proven effective for identifying seasonal patterns in stationary data. However, for non-stationary seasonal data, a differencing step is required beforehand so that the series becomes stationary before further analysis can be conducted. Thus, the parameter  $d$  not only serves to assess the presence of long memory but also provides guidance regarding the number of differencing steps needed to achieve data stationarity [22].

### 2.2.3 Autocorrelation pattern of time series data

The autocorrelation function (ACF) is used to describe the linear relationship between the current observation and previous observations in a time series. Through this function, the stability of the data can be analyzed by examining the relationship between  $Y_t$  and  $Y_{t+k}$ . For a stationary time series, the autocorrelation value at lag  $k$  is denoted by  $\hat{\rho}_k$ , which is mathematically expressed in Eq. (6) [23, 24].

$$\hat{\rho}_k = \frac{E[(Y_t - \mu)(Y_{t+k} - \mu)]}{\text{Var}(Y_t)} = \frac{\text{Cov}(Y_t, Y_{t+k})}{\text{Var}(Y_t)} \quad (6)$$

Meanwhile, the partial autocorrelation function (PACF) is used to measure the degree of correlation between  $Y_t$  and  $Y_{t+k}$  after removing the influence of the intermediate values such as  $Y_{t+1}, Y_{t+2}, \dots, Y_{t+k-1}$ . The PACF value at lag  $k$  is denoted by  $\phi_{kk}$ , as written in Eq. (7).

$$\phi_{kk} = \text{Corr}(Y_t, Y_{t+k} \mid Y_{t+1}, Y_{t+2}, \dots, Y_{t+k-1}) \quad (7)$$

The determination of the seasonal autoregressive integrated moving average (SARIMA) model order, which includes the autoregressive (AR(p)), moving average (MA(q)), seasonal autoregressive (SAR(P)), and seasonal moving average (Seasonal MA(Q)) components, is carried out by analyzing the patterns in the ACF and PACF plots. This step aids in identifying the best-fitting model for both the seasonal and non-seasonal components, as presented in Table 2.

**Table 2.** Determination of non-seasonal and seasonal model orders

Model	ACF	PACF
AR(p)	Rapid exponential decay	Cuts off after lag p
MA(q)	Cuts off after lag q	Rapid exponential decay
AR(p) or MA(p)	Cuts off after lag q	Cuts off after lag p
ARMA(p,q)	Rapid exponential decay	Rapid exponential decay
SAR(P)	Rapid exponential decay at seasonal lags	Cuts off after seasonal lag P
SMA(Q)	Cuts off after seasonal lag Q	Rapid exponential decay at seasonal lags
SAR(P) or SMA(Q)	Cuts off after seasonal lag Q	Cuts off after seasonal lag P
SARMA(P,Q)	Rapid exponential decay at seasonal lags	Rapid exponential decay at seasonal lags

Note: AR: autoregressive; MA: moving average; ARMA: autoregressive moving average; SAR: seasonal autoregressive; ACF: autocorrelation function; PACF: partial autocorrelation function.

### 2.3 Forecasting Model

The selection of SARIMAX, MLP, and the dynamic model in this study is motivated by the need to comprehensively represent different characteristics of passenger demand dynamics in urban public transportation systems. Passenger volume is influenced not only by recurring seasonal patterns and external factors such as working days and weather conditions, but also by complex non-linear interactions and short-term fluctuations that evolve over time [9, 10]. Therefore, the use of multiple forecasting paradigms allows a systematic comparison of linear, non-linear, and adaptive approaches in modeling daily passenger demand.

SARIMAX is selected as a benchmark statistical model due to its ability to explicitly model seasonal structures while incorporating exogenous variables that are relevant to public transportation demand, such as rainfall and calendar effects. Previous studies have shown that multivariate time series models provide improved forecasting performance compared to univariate approaches when external influences are present [10, 11, 23]. Moreover, the interpretability of SARIMAX makes it suitable for policy-oriented analysis in transportation systems.

However, passenger demand often exhibits non-linear responses to external factors and behavioral patterns that cannot be adequately captured by linear models. For this reason, the MLP is employed to model complex non-linear relationships among variables. Recent studies demonstrate that MLP-based models are effective in forecasting passenger volumes by learning intricate patterns directly from data, particularly in transportation and mobility contexts [12, 25].

In addition, a dynamic model is included to represent an adaptive forecasting approach in which estimates are continuously updated using the most recent observations. Such models are useful for capturing short-term variations and gradual structural changes in demand patterns, providing a practical reference for operational forecasting in dynamic urban environments [13].

By comparing these three models, this study evaluates the relative contribution of seasonal linear structures, non-linear relationships, and time-varying dynamics in forecasting daily Transjakarta passenger demand.

#### 2.3.1 Seasonal autoregressive integrated moving average with exogenous variables

An AR model is a form of regression that, instead of directly linking independent variables to the dependent variable, explains the current observation based on its past values. An AR model of order  $p$  is denoted as AR(p), with  $p = 1, 2, 3, \dots, n$ . The general form of the time series model for the AR component is presented in Eq. (8) [23, 26].

$$\phi_p(B)Y_t = a_t \quad (8)$$

The MA model is a stationary time series model in which the observation at time  $t$  is influenced by the residuals (errors) from the previous  $q$  periods, which subsequently affect the error at the current time. An MA model of order

$q$  is denoted as MA( $q$ ), with  $q = 1, 2, 3, \dots, n$ . The general form of the time series model for the MA component is presented in Eq. (9).

$$Y_t = \theta_q(B)a_t \quad (9)$$

The SARIMA model is an extension of the ARIMA model that accounts for seasonal patterns in time series data. A seasonal pattern is defined as a regularly recurring pattern at specific intervals. The SARIMAX model is an extension of SARIMA that allows external variables to influence the time series. This model combines AR components, MA components, and both seasonal and non-seasonal differencing to capture short-term and seasonal variation patterns.

In general, the SARIMA  $(p, d, q)(P, D, Q)^s$  model is used for data with seasonal patterns, where the parameters  $(p, d, q)$  represent the non-seasonal components, while  $(P, D, Q)$  represent the seasonal components with period  $s$ . The SARIMAX model then incorporates the exogenous variable  $X_t$ , which is assumed to influence the time series  $Y_t$ . Mathematically, the SARIMAX model is expressed in Eq. (10).

$$\phi_p(B)\phi_p(1-B)^d(1-B)^D Y_t = \theta_q(B)\Theta_Q(B)^s a_t + \beta_1 X_{1,t} + \beta_2 X_{2,t} + \dots + \beta_k X_{k,t} \quad (10)$$

This model allows for the simultaneous integration of internal data influences and external variables, resulting in a more accurate representation of complex time series dynamics.

### 2.3.2 Multilayer perceptron

The MLP model is one of the most commonly used artificial neural networks in time series modeling and forecasting. The MLP structure consists of an input layer, one or more hidden layers, and an output layer. Through the backpropagation algorithm, the MLP is trained in a supervised manner by computing the error at the output layer and subsequently updating the weights in the preceding layers iteratively to minimize output errors [25].

Architecturally, the MLP is a feedforward network in which data flow in one direction from the input layer to the output layer, passing through one or more hidden layers that process information and extract important features. Despite its simplicity, this model is widely used due to its ability to recognize nonlinear relationships among variables and produce highly accurate predictions.

In this model, the input layer receives the data, while the hidden layer performs nonlinear transformations using activation functions such as sigmoid or hyperbolic tangent, and the output layer provides the final linear prediction. Each neuron in a layer receives signals from all neurons in the previous layer, with connection weights  $w_{ji}$  and bias  $b_j$ . Mathematically, the output of neuron  $j$  in layer  $l$  is expressed in Eq. (11).

$$x_j^l = f \left( \sum_j w_{ji}^l x_i^{l-1} + b_j \right) \quad (11)$$

In general, the output of a neuron in the hidden layer of an MLP network can be expressed using Eq. (12) below. For clarity, let  $x = (x_1, x_2, \dots, x_M)$  denote the input vector,  $y = (y_1, y_2, \dots, y_N)$  the hidden neuron outputs, and  $z$  the final network output.

$$y_j = f \left( \sum_{i=1}^M w_{ji} x_i + b_j \right) \quad (12)$$

The output from this layer then becomes the input for the next layer until it reaches the output layer, which functions to combine all results from the hidden neurons to produce the final prediction. The final output of the network (at the output layer) can be expressed as in Eq. (13).

$$z = \sum_{k=1}^N (w_k y_k) + b \quad (13)$$

MLP is not a recurrent network, and therefore does not account for time dependence among observations. Consequently, when applied to time series data, temporal dependence must be simulated by arranging past observations  $(x_{t-1}, x_{t-2}, \dots, x_{t-M})$  as an input vector to predict the value at time  $t$ . This approach allows the MLP to capture non-linear patterns across periods even without an explicit recurrent structure.

### 2.3.3 Dynamic model

A dynamic model is an approach that accounts for changes in variable values over time. In this model, the parameters or estimates are updated periodically based on the most recent data, allowing the model to adapt to continuously evolving historical patterns [13].

One simple form of a dynamic model is the use of a moving average from several previous periods to generate a prediction for the next period. In general, the estimate at time  $t$  ( $\hat{A}_t$ ) is calculated as the average of previous observations within a specified time interval, for instance on a weekly basis, which can be formulated as in Eq. (14) below.

$$\hat{A}_t = \frac{1}{n} (A_{t-7} + A_{t-14} + \dots + A_{(t-n) \times 7}) \quad (14)$$

where,  $n$  represents the number of historical periods used as the basis for calculation. Selecting an optimal value of  $n$  is a crucial aspect of dynamic models. A value that is too small may cause the model to become overly sensitive to short-term fluctuations, whereas a value that is too large may obscure recent changes in the data. Therefore, the parameter  $n$  can be determined by minimizing prediction errors, such as the Mean Squared Error (MSE), to achieve a balance between model stability and its ability to adapt to changes in the data.

## 2.4 Metric Evaluation

MAPE is an evaluation metric that measures the average absolute difference between predicted values and actual values. The MAPE value is expressed as a percentage of the actual value, with the following categories: MAPE < 10% is classified as excellent, 10–20% as good, 20–50% as acceptable, and >50% as unacceptable. MAPE is used in forecasting evaluation to assess the level of accuracy between predicted results and actual data, and it can be calculated using the formula in Eq. (15) below [26–28].

$$MAPE = \frac{1}{n} \sum_{t=1}^n \left| \frac{y_t - \hat{y}_t}{y_t} \right| \times 100\% \quad (15)$$

where,  $y_t$  is the actual value,  $\hat{y}_t$  is the predicted value,  $n$  is the number of observations, and  $t$  indicates the observation period.

## 2.5 Research Procedures

The research procedures conducted in this study are described as follows:

- (1). Obtaining the data to be used, namely the daily number of Transjakarta passengers and the related exogenous variables, which include daily rainfall (mm), weekday (working day vs. weekend), and national holidays from January 1, 2023 to April 30, 2025.
- (2). Identifying the characteristics of the data by performing data stationarization using differencing based on the GPH test results, identifying seasonal patterns using spectral regression, and examining autocorrelation through the ACF and PACF plots.
- (3). Forecasting the number of Transjakarta passengers by implementing the SARIMAX, MLP, and dynamic model approaches.
- (4). Evaluating and comparing the performance of the three models using the MAPE metric to determine the best-performing model.
- (5). Drawing conclusions from the best-performing model to predict the number of Transjakarta passengers and presenting the final forecasting results.

## 3 Results

### 3.1 Data Characteristics

#### 3.1.1 Data stationarization

Based on the results of the GPH test conducted using Microsoft Excel, the estimated value of  $d$  is 0.1898580639. This value falls within the range  $0 < d < 0.5$ , indicating that the data exhibit stationary longmemory characteristics.

#### 3.1.2 Seasonal pattern identification

Based on the spectral regression analysis performed using Microsoft Excel, the frequency with the largest periodogram value was obtained at  $k = 122$  with  $I^{(122)}(\omega_{(122)}) = 6535356717122.05$ . The calculated Fourier coefficient produced an  $F_{\text{statistic}}$  of 67.76207, while the critical value from the  $F_{\text{table}}$  was 3.006.

Since the  $F_{\text{statistic}}$  is greater than the critical value at the 5 percent significance level,  $H_0$  is rejected. Therefore, at the 122nd frequency, there is a significant seasonal component, indicating that the data contain a seasonal pattern at

that frequency. The frequency was then further tested using Fisher's  $T$  test statistic to determine the specific seasonal period in which the significant pattern appears. The results of the calculation are presented in Table 3.

Based on the analysis, since  $T > g_\alpha$  at the 5 percent significance level,  $H_0$  is rejected. Thus, the periodicity at the 122nd frequency is declared significant. The seasonal period at this frequency can be calculated using the formula  $P = \frac{2\pi}{\omega}$ , resulting in a seasonal period of 7. This indicates that the seasonal pattern in the Transjakarta passenger data repeats every one week.

**Table 3.** Results of fisher's  $T$  test

$T$	$g_\alpha$
0.4571595464	0.0211131

### 3.1.3 Autocorrelation pattern

Based on the analysis of the ACF plot in Figure 1, the pattern shows a tails-off structure, characterized by many significant autocorrelation lags lying outside the confidence bounds. This pattern strongly indicates that the Transjakarta passenger data are not stationary in mean and contain a trend, therefore requiring non-seasonal differencing with  $d$  equal to 1. After the differencing process, the ACF and PACF plots were reanalyzed to identify other model orders.

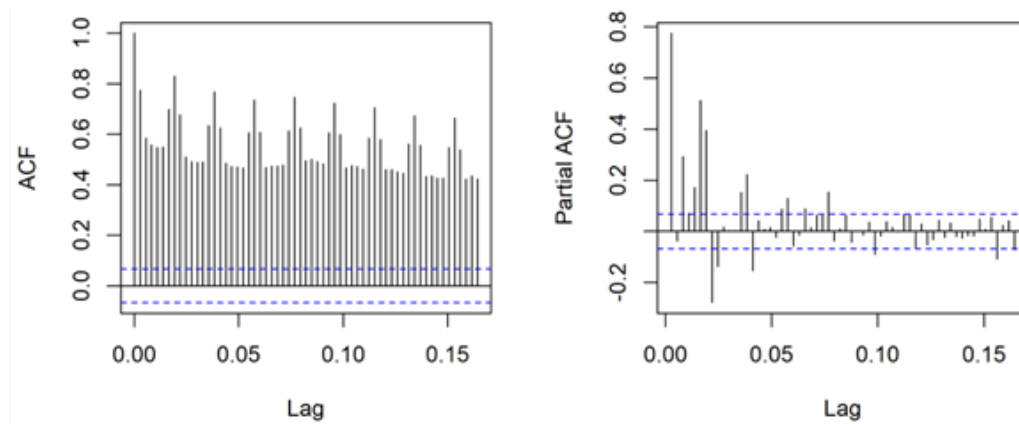


**Figure 1.** Autocorrelation function (ACF) and partial autocorrelation function (PACF) plots before differencing

The main focus of the plots after differencing is on the seasonal component based on Figure 2. The PACF plot shows a very clear cut-off pattern at the seasonal lags, with significant spikes at lag 7 and lag 14 that then decline and become insignificant at the subsequent multiples of 7. This cut-off pattern after two seasonal lags is characteristic of a seasonal AR model of order two ( $P = 2$ ). Since the SAR(2) model already captures the seasonal pattern effectively, seasonal differencing is not required, resulting in  $D$  equal to 0. This finding is supported by the ACF plot, which shows a tails-off pattern at seasonal lags (7, 14, 21, and so on), reflecting an SAR process. This confirms that the Seasonal Moving Average order is 0.

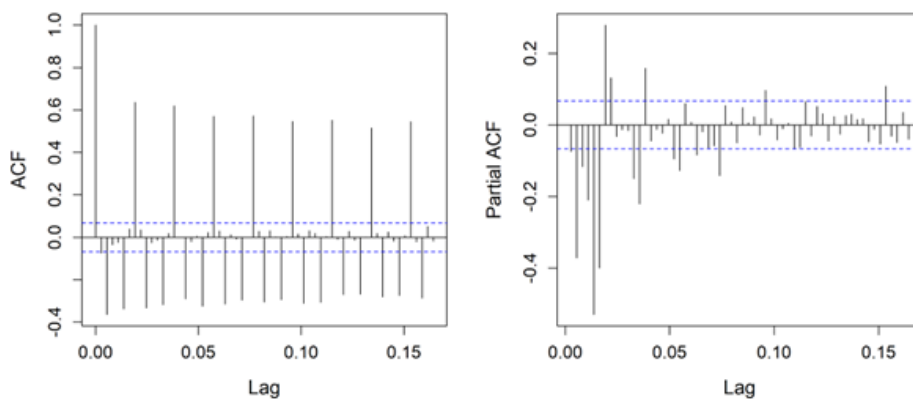


**Figure 2.** Autocorrelation function (ACF) and partial autocorrelation function (PACF) plots after differencing

For the non-seasonal component, the PACF plot after differencing shows several statistically significant spikes. The dominant non-seasonal pattern appears at lag 1 and lag 2, where two negative spikes are present. This strongly indicates the presence of an AR component, suggesting orders  $p$  equal to 1 or  $p$  equal to 2 as the main candidates. Meanwhile, the ACF plot after differencing also shows several significant early lags, suggesting the presence of an MA component, therefore,  $q$  equals to 1, 2, or 3 must also be considered.

Therefore, the candidate models were evaluated using the basic structure SARIMA  $(p, 1, q)(2, 0, 0)^T$ , with various identified combinations of  $p$  and  $q$ , such as (1, 2), (2, 1), (1, 1), (0, 2), and (0, 3), tested to determine the most optimal combination. The preliminary SARIMA candidate models obtained are shown in Table 4 below.

**Table 4.** Preliminary seasonal autoregressive integrated moving average (SARIMA) models

Model
SARIMA (1, 1, 2)(2, 0, 0) <sup>T</sup>
SARIMA (2, 1, 1)(2, 0, 0) <sup>T</sup>
SARIMA (1, 1, 1)(2, 0, 0) <sup>T</sup>
SARIMA (0, 1, 2)(2, 0, 0) <sup>T</sup>
SARIMA (0, 1, 3)(2, 0, 0) <sup>T</sup>

### 3.2 Forecasting Models

#### 3.2.1 Seasonal autoregressive integrated moving average with exogenous variables

Based on the SARIMAX model analysis conducted using R software, the Akaike information criterion (AIC) values for several model combinations were obtained, as shown in Table 5.

**Table 5.** Seasonal autoregressive integrated moving average with exogenous variables (SARIMAX) model combinations

Model	Akaike Information Criterion (AIC)
SARIMAX (1, 1, 2)(2, 0, 0) <sup>T</sup>	17679.15
SARIMAX (2, 1, 1)(2, 0, 0) <sup>T</sup>	17681.92
SARIMAX (1, 1, 1)(2, 0, 0) <sup>T</sup>	17689.67
SARIMAX (0, 1, 2)(2, 0, 0) <sup>T</sup>	17698.09
SARIMAX (0, 1, 3)(2, 0, 0) <sup>T</sup>	17699.54

Based on the evaluation of several SARIMAX model combinations, the SARIMAX  $(1, 1, 2)(2, 0, 0)^T$  model was found to have the lowest AIC value of 17679.15. A lower AIC value indicates a better balance between model fit and model complexity compared to the other alternatives. The next step is to generate forecasts using the selected model. The forecasting results are shown in Figure 3, which presents a comparison between the actual values and the predicted values. The MAPE of 33.345 percent indicates that the prediction accuracy of the model falls within the moderate category.

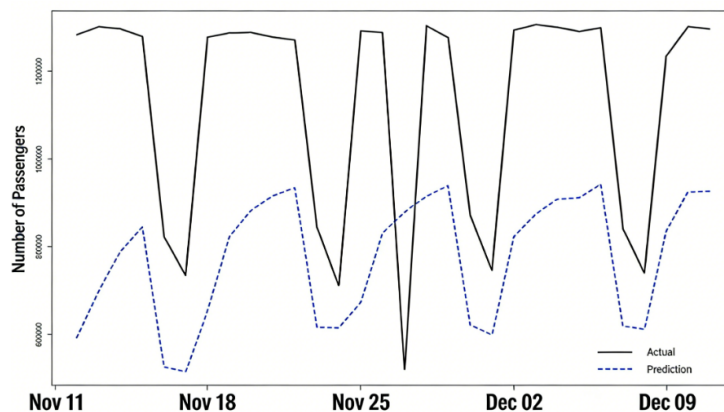


**Figure 3.** Comparison of actual and predicted values for the seasonal autoregressive integrated moving average with exogenous variables (SARIMAX) model

Overall, these results show that the SARIMAX model is not yet able to capture the data patterns effectively. Although the predicted series closely resembles the actual pattern and successfully follows the recurring seasonal trend, the accuracy remains low because of substantial differences between predicted and actual values in several periods. This indicates that the model struggles to represent the non-linear relationships and sharp fluctuations present in the passenger data. Therefore, alternative methods capable of capturing non-linear relationships and producing higher accuracy are needed.

### 3.2.2 Multilayer perceptron

Before training the model, the key parameters of the MLP method were determined. These parameters were selected to obtain an optimal model configuration capable of generating accurate predictions. The parameters used in this study are presented in Table 6.

**Table 6.** Configuration of the neural network model

Parameter	Jumlah
Total Layer	3 layer
Input Layer	1 layer (10 neuron)
Hidden Layer	1 layer (128 neuron)
Output Layer	1 layer (1 neuron)
Epoch	100
Activation	ReLU
Optimizer	Adam

After determining the main parameters of the MLP model as shown in Table 6, the next step was to train and test the model to obtain forecasting results. The predictions produced by the MLP model are shown in Figure 4, which compares the actual values with the predicted values. The MAPE of 8.547 percent indicates that the prediction error is low, meaning that the MLP model can be categorized as having good accuracy for this study.

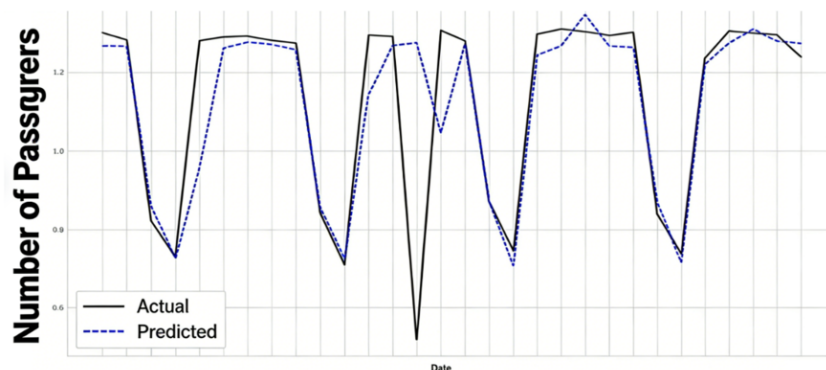


**Figure 4.** Comparison of actual and predicted values for the multilayer perceptron (MLP) Model

Overall, these results show that the MLP model is able to capture the data patterns effectively and produce predictions that closely match the actual values. This indicates that neural network-based approaches are effective for modeling data with complex and non-linear patterns. However, despite the low prediction error, there are still small deviations in several periods, which may be caused by fluctuations that are not fully represented by the model. Therefore, in the next stage, the performance of the MLP model will be compared with other forecasting methods to obtain the most optimal prediction results.

### 3.2.3 Dynamic model

The dynamic model approach was applied to enhance the ability of the model to adapt to changes in data patterns over time. In this approach, the model is trained periodically using the most recent historical data before generating predictions for the subsequent period. As a result, the model parameters are continuously updated based on the latest information, enabling more adaptive and accurate forecasts.

To determine the optimal length of historical data, tests were conducted using window sizes ranging from 1 to 28 weeks. The results of these tests are presented in Figure 5, which displays the training root mean squared error (RMSE) for each value of  $n$ .

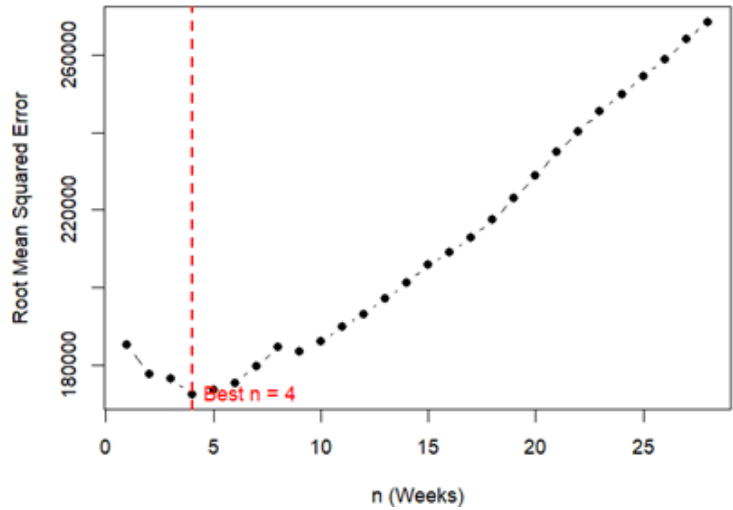


**Figure 5.** Comparison of training root mean squared error (RMSE) based on number of weeks ( $n$ )

The results show that the MSE pattern forms a U-shaped curve, where the RMSE decreases as the number of weeks increases until it reaches a minimum, then increases again. The lowest training RMSE of 172337.3 was obtained when using  $n$  equal to 4 weeks; thus, this value was selected as the optimal configuration for the dynamic model. This indicates that using 4 weeks of historical data provides the best balance between capturing long-term stability and detecting short-term variation in the data.

Based on Figure 6, it is evident that although the dynamic model is able to follow the general trend of the actual data, there are considerable discrepancies in several periods. This shows that the daily fluctuations in passenger volume are not fully captured by the model. In addition, evaluation of the test data shows that the model with  $n$  equal to 4 produces a MAPE of 37.754 percent for the 30-day forecasting horizon. This value indicates that the prediction accuracy is still moderate, but the dynamic model remains capable of providing a reasonably representative overview of the overall passenger volume trend.

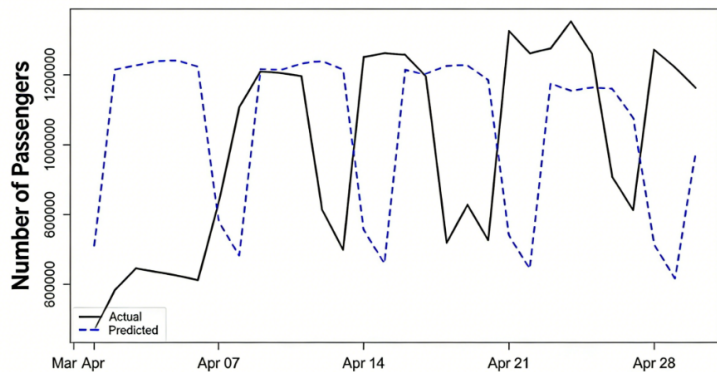


**Figure 6.** Comparison of actual and predicted values for the dynamic model

### 3.3 Metric Evaluation

To evaluate the performance of each model in generating forecasts, a comparison of the MAPE values was conducted for the SARIMAX, the MLP, and the dynamic model over a 30-day forecasting horizon. This comparison aims to identify the model with the lowest relative prediction error and to assess the extent to which each approach consistently represents the actual data patterns within the specified prediction period, as presented in Table 7.

Based on the evaluation results using MAPE values, the MLP model achieves a MAPE of 8.547 percent, which falls into the very good category. This indicates that the MLP model is capable of producing predictions with very small errors and demonstrates a strong ability to accurately capture the actual data patterns. As a result, the daily passenger demand forecasts generated by this model can provide a reliable basis for short-term planning and operational considerations in passenger transportation systems.

**Table 7.** Comparison of mean absolute percentage error (MAPE) values for the three models

Model	MAPE
SARIMAX	33.345%
MLP	8.547%
Dynamic Model	37.754%

Note: SARIMAX: seasonal autoregressive integrated moving average with exogenous variables; MLP: multi-Layer perceptron neural network.

Meanwhile, the SARIMAX model has a MAPE of 33.345 percent, and the dynamic model yields 37.754 percent, both of which fall into the fair category. This means that although these two models can still represent the general pattern of the data, their accuracy is considerably lower than that of the MLP model. In practical terms, error levels of this magnitude may result in noticeable discrepancies between predicted and actual passenger demand, potentially affecting the reliability of the forecasts for short-term planning and operational analysis. Overall, these results highlight the comparative advantage of the MLP model for the 30-day forecasting horizon, particularly in capturing complex and nonlinear patterns in daily passenger demand.

#### 4 Discussion

The empirical results indicate clear differences in the forecasting performance of the three modeling approaches considered, reflecting their distinct capabilities in representing the temporal structure and external influences of daily urban bus ridership. The comparison confirms that incorporating calendar and weather-related information, together with flexible functional forms, is important for capturing short-term demand variability in large-scale public transport systems [11, 12].

The SARIMAX model was able to represent the dominant weekly seasonal pattern and the effects of observable exogenous variables, demonstrating its suitability for modeling regular and interpretable demand structures. However, its MAPE of 33.345% indicates limited accuracy in the presence of sharp day-to-day fluctuations and non-linear interactions between demand and external conditions. This limitation is consistent with previous findings reported by Ikasari et al. [14], who observed that simpler time series models such as SES provide only moderate accuracy when applied to Transjakarta ridership data and do not explicitly account for exogenous or non-linear effects. These results suggest that linear statistical models alone may be insufficient for operational forecasting in environments characterized by irregular and rapidly changing demand patterns.

In contrast, the MLP model achieved substantially higher accuracy, with a MAPE of 8.547%, indicating a strong ability to learn complex and non-linear relationships between ridership and its influencing factors [12, 21]. This performance suggests that data-driven non-linear models are better suited for short-term operational forecasting, particularly in settings where demand is affected by multiple interacting factors such as working schedules, holidays, and weather conditions. The remaining deviations observed in certain periods are likely associated with unpredictable events or behavioral changes that are not fully captured by the available explanatory variables, pointing to the potential value of incorporating additional real-time or contextual information in future applications.

The dynamic moving-window model provided a simple adaptive benchmark by updating predictions based on recent observations. Although it followed the general trend of the data, its relatively high MAPE of 37.754% indicates limited suitability for precise short-term forecasting. This result reflects the inherent trade-off of moving-average-based approaches, which offer robustness and simplicity but lack the capacity to represent complex non-linear dynamics and interactions [13].

From an intelligent transportation systems perspective, these findings highlight the complementary roles of different modeling approaches. Statistical models such as SARIMAX can support strategic analysis and interpretation of seasonal and policy-related effects, while machine learning models such as MLP are more appropriate for short-term operational forecasting and demand-responsive service management. The dynamic model, although less accurate, may still serve as a lightweight tool for rapid approximation or baseline comparison in resource-constrained environments.

Overall, the results support the view that effective demand forecasting in urban public transportation requires both the integration of external contextual information and the use of flexible modeling techniques capable of representing non-linear behavior. The improved accuracy obtained with the MLP model suggests that such approaches can contribute to more informed service planning, fleet allocation, and timetable adjustment in systems such as Transjakarta. Future research may explore hybrid frameworks that combine the interpretability of statistical models with the predictive strength of neural networks, as well as the integration of real-time data sources, to further enhance forecasting reliability and operational relevance.

## 5 Conclusions

The analysis confirms that daily Transjakarta ridership exhibits both regular weekly seasonality and pronounced short-term variability driven by calendar and external conditions. The results indicate that the MLP model achieves the highest forecasting accuracy, with a MAPE of 8.547%, reflecting its ability to capture non-linear relationships and irregular demand fluctuations. The SARIMAX model, while effective in representing seasonal structures and incorporating exogenous variables, shows only moderate predictive performance, and the dynamic moving-window model is primarily suited to tracking general trends rather than producing precise short-term forecasts.

These findings suggest that linear and purely adaptive models alone are insufficient for representing the complex demand dynamics observed in large urban public transportation systems. Non-linear data-driven approaches provide a more suitable basis for short-term demand forecasting, particularly in operational contexts where passenger volumes are influenced by interacting calendar, behavioral, and environmental factors.

From an intelligent transportation systems perspective, the improved accuracy obtained with non-linear models supports their use in demand-aware service planning, fleet allocation, and timetable adjustment. More reliable short-term forecasts can contribute to better alignment between service supply and passenger demand, potentially improving service efficiency and passenger experience in high-volume transit systems such as Transjakarta.

Several limitations should be noted. The analysis relies on a limited set of exogenous variables and does not account for real-time information, special events, or policy interventions that may also influence travel behavior. Future research may therefore consider hybrid modeling frameworks that combine statistical and machine learning approaches, as well as the integration of real-time and contextual data sources, to further enhance forecasting robustness and operational relevance.

### Author Contributions

Conceptualization, H.K. and F.O.W.; methodology, G.D.; software, H.K.; validation, H.K., F.O.W., and G.D.; formal analysis, F.O.W.; investigation, H.K.; resources, F.O.W.; data curation, H.K.; writing—original draft preparation, H.K. and F.O.W.; writing—review and editing, H.K. and F.O.W.; visualization, F.O.W.; supervision, G.D.; project administration, H.K. and F.O.W. All authors have read and agreed to the published version of the manuscript.

### Data Availability

The data used to support the research findings are available from the corresponding author upon request.

### Conflicts of Interest

The authors declare no conflicts of interest.

### References

- [1] T. Afrin and N. Yodo, "A survey of road traffic congestion measures towards a sustainable and resilient transportation system," *Sustainability*, vol. 12, no. 11, p. 4660, 2020. <https://doi.org/10.3390/su12114660>
- [2] A. Khoirunni'mah and D. F. Brilianti, "The effect of congestion on productivity in the Semarang urban area," *J. Sci. Res. Educ. Technol.*, vol. 4, no. 1, 2025. <https://jsret.knpub.com/index.php/jrest/article/view/652>
- [3] H. S. Hasibuan, C. T. Permana, B. N. Elizandri, F. W. Asrofani, R. Harmain, and D. P. Putra, "Sustainable mobility in Jakarta's Transit-Oriented development: Energy savings and emission reduction strategies," *Sustainability*, vol. 17, no. 23, p. 10603, 2025. <https://doi.org/10.3390/su172310603>
- [4] A. A. A. Shiddiqi, D. Sutjiningsih, T. Tjahjono, L. Darmajanti, and G. B. Suprayoga, "Modal shift in public transport under fiscal-based policies scenarios for Jakarta," *Int. J. Technol. (IJTech)*, vol. 15, no. 6, pp. 1862–1872, 2024. <https://doi.org/10.14716/ijtech.v15i6.5723>
- [5] M. Gewati, "Beroperasi 2004, Transjakarta kini miliki lintasan BRT terpanjang di dunia," 2019. <https://kilasdaerah.kompas.com/dki-jakarta/read/2019/10/26/12321851/beroperasi.2004.transjakarta.kini.miliki.lintasan.brt.terpanjang.di.dunia>
- [6] R. F. Regar and A. H. Maulana, "Jumlah penumpang Transjakarta capai 371 juta sepanjang 2024, naik hampir 2 kali lipat dari 2022," 2025. <https://megapolitan.kompas.com/read/2025/02/06/16043271/jumlah-penumpang-transjakarta-capai-371-juta-sepanjang-2024-naik-hampir-2>
- [7] Dewan Perwakilan Rakyat Daerah Provinsi Daerah Khusus Ibukota Jakarta, "Perluasan rute Transjakarta," 2025. <https://dprd-dkijakartaprov.go.id/perluasan-rute-transjakarta/>
- [8] P. Lin, J. Weng, D. K. Brands, H. Qian, and B. Yin, "Analysing the relationship between weather, built environment, and public transport ridership," *IET Intell. Transp. Syst.*, vol. 14, no. 14, pp. 1946–1954, 2021. <https://doi.org/10.1049/iet-its.2020.0469>

- [9] E. E. Etu, L. Monplaisir, S. Masoud, S. Arslanturk, J. Emakhu, I. Tenebe, J. B. Miller, T. Hagerman, D. Jordan, and S. Krupp, "A comparison of univariate and multivariate forecasting models predicting emergency department patient arrivals during the COVID-19 pandemic," *Healthcare*, vol. 10, no. 6, 2022. <https://doi.org/10.3390/healthcare10061120>
- [10] V. A. Alencar, L. R. Pessamilio, F. Rooke, H. S. Bernardino, and A. B. Vieira, "Forecasting the carsharing service demand using uni and multivariable models," *J. Internet Serv. Appl.*, vol. 12, no. 1, p. 4, 2021. <https://doi.org/10.1186/s13174-021-00137-8>
- [11] O. I. Rebrin, L. A. Zakharov, L. A. Derksen, and V. I. Derksen, "Modeling and forecasting the parameters of a railroad transport system," *J. Phys.: Conf. Ser.*, vol. 1679, no. 3, p. 032018, 2020. <https://doi.org/10.1088/1742-6596/1679/3/032018>
- [12] H. Lu, B. Guo, Z. Zhang, and W. Gu, "Research on a highway passenger volume prediction model based on a multilayer perceptron neural network," *Appl. Sci.*, vol. 14, no. 8, p. 3438, 2024. <https://doi.org/10.3390/app14083438>
- [13] W. Whitt and X. Zhang, "Forecasting arrivals and occupancy levels in an emergency department," *Oper. Res. Health Care*, vol. 21, pp. 1–18, 2019. <https://doi.org/10.1016/j.orhc.2019.01.002>
- [14] D. Ikasari, R. A. Permana, and Widiastuti, "Prediction in the number of passengers on Transjakarta public transportation using the single exponential smoothing method," *Int. Res. J. Adv. Eng. Sci.*, vol. 9, no. 2, pp. 146–153, 2024. <https://irjaes.com/wp-content/uploads/2024/06/IRJAES-V9N2P197Y24.pdf>
- [15] Dinas Komunikasi, Informatika dan Statistik Provinsi Daerah Khusus Ibukota Jakarta, "Jumlah penumpang angkutan umum yang terlayani perhari," 2025. [https://satudata.jakarta.go.id/open-data/detail?kategori=database&page\\_url=jumlah-penumpang-angkutan-umum-yang-terlayani-perhari&data\\_no=1](https://satudata.jakarta.go.id/open-data/detail?kategori=database&page_url=jumlah-penumpang-angkutan-umum-yang-terlayani-perhari&data_no=1)
- [16] Open-Meteo, "Historical weather API," 2025. <https://open-meteo.com/en/docs/historical-weather-api>
- [17] JDIH Kementerian Koordinator Bidang Infrastruktur dan Pembangunan Kewilayahan, "Kalender libur nasional dan cuti bersama tahun 2023," 2022. <https://jdih.kemenkoinfra.go.id/infografis/kalender-libur-nasional-dan-cuti-bersama-tahun-2023>
- [18] Kementerian Koordinator Bidang Pembangunan Manusia dan Kebudayaan, "Pemerintah tetapkan hari libur nasional dan cuti bersama tahun 2024," 2023. <https://www.kemenkopmk.go.id/pemerintah-tetapkan-hari-libur-nasional-dan-cuti-bersama-tahun-2024>
- [19] Kementerian Koordinator Bidang Infrastruktur dan Pembangunan Kewilayahan, "Informasi hukum infografis libur nasional dan cuti bersama 2025," 2025. <https://jdih.kemenkoinfra.go.id/infografis/libur-nasional-dan-cuti-bersama-2025>
- [20] D. Devianto, E. Wahyuni, M. Maiyastri, and M. Yollanda, "The seasonal model of chili price movement with the effect of long memory and exogenous variables for improving time series model accuracy," *Front. Appl. Math. Stat.*, vol. 10, p. 1408381, 2024. <https://doi.org/10.3389/fams.2024.1408381>
- [21] S. I. Christienova, E. W. Pratiwi, and G. Darmawan, "Perbandingan model peramalan Singular Spectrum Analysis (SSA) dan Fourier Series Analysis (FSA) pada data suhu udara di Surabaya," *Berk. MIPA*, vol. 25, no. 1, pp. 94–106, 2018. <https://jurnal.ugm.ac.id/bimipa/article/view/27470>
- [22] G. Darmawan, S. Mulyani, and Sudartianto, "Pengujian pola musiman pada data deret waktu dengan menggunakan regresi spektral," in *Prosiding Seminar Nasional Statistika*, 2012, pp. 1–10. <https://prosidin.g.statistics.unpad.ac.id/?journal=prosidingSNS&page=article&op=view&path%5B%5D=234>
- [23] Z. Zeinawaqi and A. A. Dzikrullah, "Factors affecting the number of domestic flights in Indonesia during Covid-19 pandemic using SARIMAX method," *J. Matem. Sains Komput.*, vol. 21, no. 1, pp. 1–9, 2024. <https://doi.org/10.20956/j.v21i1.34557>
- [24] T. Peychinov, A. Karaivanova, and T. Mecheva, "Predicting traffic load data: ARIMA and SARIMA comparison," *Eng. Proc.*, vol. 100, no. 1, p. 29, 2025. <https://doi.org/10.3390/engproc2025100029>
- [25] A. Lazcano, M. A. Jaramillo-Morán, and J. E. Sandubete, "Back to basics: The power of the multilayer perceptron in financial time series forecasting," *Mathematics*, vol. 12, no. 12, p. 1920, 2024. <https://doi.org/10.3390/math12121920>
- [26] F. R. Alharbi and D. Csala, "A seasonal autoregressive integrated moving average with exogenous factors (SARIMAX) forecasting model-based time series approach," *Inventions*, vol. 7, no. 4, p. 94, 2022. <https://doi.org/10.3390/inventions7040094>
- [27] D. Chicco, M. J. Warrens, and G. Jurman, "The coefficient of determination R-squared is more informative than SMAPE, MAE, MAPE, MSE and RMSE in regression analysis evaluation," *PeerJ Comput. Sci.*, vol. 7, p. e623, 2021. <http://dx.doi.org/10.7717/peerj-cs.623>
- [28] L. F. L. Blanco and R. W. M. Hanco, "Modeling and forecasting international tourism demand in Puno-Peru," *Rev. Bras. Pesq. Turismo*, vol. 14, no. 1, pp. 34–55, 2020. <https://www.redalyc.org/jatsRepo/5041/504162911003/html/index.html>